A Piece-wise Linearized Transformer Winding Model for the Analysis of Internal Voltage Propagation

Theocharis, Andreas; Popov, Marjan

DOI
10.1109/PTC.2019.8810920

Publication date
2019

Document Version
Final published version

Published in
2019 IEEE Milan PowerTech

A Piece-wise Linearized Transformer Winding Model for the Analysis of Internal Voltage Propagation

Andreas Theocharis
Department of Engineering and Physics
Karlstad University, KAU
Karlstad, Sweden
andreas.theocharis@kau.se

Marjan Popov
Department of Electrical Sustainable Energy
Technical University of Delft, TUDelft
Delft, The Netherlands
M.Popov@tudelft.nl

***Abstract*—In this paper, a piece-wise linearized transformer winding model is proposed for transient internal voltage distribution computations. In particular, the model is based on the linearization of the primitive non-linear, frequency dependent and invariant matrix of voltage distribution factors. This primitive matrix is utilized as a pattern from which, for any specific switching event and its frequency spectrum, the piece-wise linearized matrix of voltage distribution factors can be computed. In this manner, a unified black-box to lumped-parameters combined transformer model successfully bypasses the need of geometrical data. The computations are also significantly reduced. The model is verified by measurements on a three-phase distribution transformer.**

***Index Terms*-- Lumped-parameters model, overvoltages, internal voltage distribution, transformer, transients, modelling.**

I. INTRODUCTION

Cigre Joint Working Group (A2/C4.39) concluded that when the natural frequency of a surge impulse matches the natural frequency of the system in which the transformer participates, a resonance in the system occurs [1]-[15]. As a consequence, very high internal overvoltages and finally insulation failures may occur when the surge impulses at transformer terminals cause internal transformer resonances [8], [9]. Generally, three types of transformer models are used for switching transient events; the white-box models, the grey-box models and the black-box models.

The white-box models can be classified as transmission line and lumped-parameters models. Transmission line models require very detailed design information of the transformer, they are time consuming and are considered as an approach for very fast transients and voltage propagation studies [16]-[20]. The lumped-parameter models are based on transformer geometrical data, which can be used for the simulation of lightning impulses [21]-[24] and switching fast transients [8], [25]-[28]. Moreover, they are used to study the interaction of the transformer with the surrounding network and to evaluate the internal voltage distribution [8], [29]. By contrast, the parameters of the black-box models are computed by using external input and output data. They are used to analyze the transformer interaction with the system and to study transferred overvoltages between terminals. They are based on frequency measurements of the terminals admittance matrix [4]-[6], [10]-[15], [30]. If an internal into the winding measuring point is provided, this modelling approach can be used for internal voltage computation [31]. The grey-box approach compromises the above concepts and the parameters are determined by using geometrical and measured data.

The idea to combine black box transformer terminals models, already implemented into EMTP-based simulators, to suitable lumped-parameter transformer winding models for wide band terminal and internal switching transient overvoltage studies is a promising method for a unified transformer model [32], [33]. The terminal voltages computed from a black box model are used as inputs for the lumped-parameter winding model. Nevertheless, although there is no need for geometrical data of black-box model, the drawback for detailed geometrical data remains in order to define the lumped parameters of the winding model. Moreover, the computation time could be significant because in the first step, the solution of the black-box model provides terminal currents and voltages and in the next step, the solution of the lumped-parameters model provides internal voltages. In order to overcome these disadvantages, a method for direct internal voltage distribution computation has been established, which is based on the matrix of voltage distribution factors in [34]. That matrix reflects the non-linear frequency dependency of the winding's parameters. Hence, it needs to be determined for each particular frequency vector that stands during a particular switching event. However, the winding follows the time-invariance property. Consequently, the frequency dependency pattern remains unchangeable, no matter what the frequency vector of the switching event is. The time-invariance property of the winding allows the piece-wise linearization of the matrix that consists the voltage distribution factors, for which a piece-wise linearized transformer winding model is based upon.

In this paper, a piece-wise linearized transformer winding

This work was supported in part by the KPN project "Electromagnetic transients in future power systems (ref. 207160/E20)" financed by the Norwegian Research Council RENERGI program and a consortium of industry partners led by SINTEF Energy Research, Norway and Siemens AG.

978-1-5386-4722-6/19/$31.00 ©2019 IEEE

model is developed. In particular, the matrix of voltage distribution factors in [34] is re-defined as a primitive matrix determined over an arbitrary primitive frequency vector. Any other voltage distribution factors matrix over the frequency vector that governs a particular switching event is computed by linearizing the primitive matrix. In this manner, the need of detailed geometrical data for the unified black-box to lumped-parameters models is avoided as long as the primitive matrix is known through a valid method. The second advantage is that the unified model computations are significantly reduced. The method is verified by laboratory measurements performed on a three-phase distribution transformer.

II. THE LINEARIZED MODEL

A. Equivalent circuit of the winding non-linear model

The transformer winding model is derived with respect to winding geometry and other structural features such as earthed points and winding's adjacency with the core [35]. In Fig. 1, the final circuit is presented as a connection of lumped-parameter blocks. Each block represents a division of the winding that could be one turn or a group of turns of the winding. The values of the lumped parameters of the blocks are computed by suitable methods as those given in [36]. For the equivalent circuit in Fig. 1, L_{si}, C_{si} and R_{si}, Y_{si} are the self-inductance, series capacitance and the associated series resistance and conductance as well as C_{shi} and Y_{shi} are the associated shunt capacitance and conductance to "reference" of the ith block. The mutual inductive components are not shown in the figure for simplicity. Usually, in order to avoid matrices of extremely large dimensions and long computation times, one division corresponds to a number of winding's turns e.g. one coil.

B. Model analysis description

The winding model analysis is based on the usage of the amplification factor as it is presented in [34]. The amplification factor depends on the angular frequency ω and the winding structure. It can be computed in terms of the impedance matrix of the equivalent circuit shown in Fig. 1. The amplification factor $N_{1i,1}(\omega)$ between the nodes "1" and "i" in respect to the input at terminal "1" is determined as

$$N_{1i,1}(\omega) = 1 - \frac{\mathrm{Z}_{i1}(\omega)}{\mathrm{Z}_{11}(\omega)} \tag{1}$$

where $Z_{i1}(\omega)$ and $Z_{11}(\omega)$ are elements of the nxn impedance matrix $\left[Z_{ij}(\omega)\right]$ (i=1,..,n and j=1,…,n) of the winding model illustrated in Fig.1. In the same manner, the amplification factor $N_{nm,n}(\omega)$ between the nodes "n" and "i" with respect to the input at terminal "n" is determined as

$$N_{ni,n}(\omega) = 1 - \frac{\mathrm{Z}_{in}(\omega)}{\mathrm{Z}_{nn}(\omega)}. \tag{2}$$

The internal node voltage vector $\left[e_i(\omega)\right]$ is computed by

$$\left[e_i(\omega)\right] = \left[\left[T_{i,1}(\omega)\right] \quad \left[T_{i,n}(\omega)\right]\right] \begin{bmatrix} e_1(\omega) \\ e_n(\omega) \end{bmatrix} \tag{3}$$

for i=2,…,n-1 and where $\left[e_1(\omega) \quad e_n(\omega)\right]^T$ is the transposed input vector at terminals "1" and "n" according to Fig.1. The elements in the (n-2)x1 size matrices $\left[T_{i,1}(\omega)\right]$ and $\left[T_{i,n}(\omega)\right]$ of the (n-2)x2 $\left[\left[T_{i,1}(\omega)\right] \quad \left[T_{i,n}(\omega)\right]\right]$ transformation matrix are functions of the non-linear frequency depended amplification factors, which can be computed through the elements of the nxn impedance matrix $\left[Z_{ij}(\omega)\right]$ of the equivalent model in Fig.1. The $\left[\left[T_{i,1}(\omega)\right] \quad \left[T_{i,n}(\omega)\right]\right]$ matrix is called as the matrix of voltage distribution factors and expresses the voltage distribution at the internal n-2 nodes along the winding in respect of the two input voltages $e_1(\omega)$ and $e_n(\omega)$ [34].

C. Computation of the matrix of voltage distribution factors

The computation of the voltage distribution factors' matrix is accomplished through successful computation of the impedance matrix of the equivalent circuit in Fig. 1. In [36], an extensive investigation about the role of lumped parameters shown in Fig. 1 is presented. The magnetic core influence, with both frequency dependent or constant parameters, and the method of zero magnetic flux penetration into the core are compared. The comparison, as it is presented in [36] in terms of the winding terminal impedance from terminals"1" and "n", indicates that the assumption of zero magnetic flux penetration into the core is valid from some tens of kilohertz and above. Hence, the impedance matrix is computed as

$$\left[Z_{ij}(\omega)\right] = \left(\left[\mathrm{B}_{ij}(\omega)\right] + \left[\Gamma_{ij}(\omega)\right]\right)^{-1} \tag{4}$$

where the matrices $\left[\mathrm{B}_{ij}(\omega)\right]$ and $\left[\Gamma_{ij}(\omega)\right]$ are given by

$$\left[\mathrm{B}_{ij}(\omega)\right] = (\omega \tan\delta + j\omega)\left[C_{ij}\right] \tag{5}$$

$$\left[\Gamma_{ij}(\omega)\right] = \left[k_{ij}\right]\left\{\left(\sqrt{2\omega/\sigma\mu_0 d^2} + j\omega\right)\left[L_{ij}\right]\right\}^{-1}\left[k_{ij}\right]^{\mathrm{T}}. \tag{6}$$

In (5) and (6), tanδ is the loss tangent of the insulation dielectric losses factor, $\left[C_{ij}\right]$ is the nodal capacitances matrix, $\left[k_{ij}\right]$ is Kron's invariant transformation matrix. $\left[L_{ij}\right]$ is the inductances matrix in which core effects are included, d is the distance between the turns of the same coil, σ is the conductor conductivity and μ_0 is the magnetic permeability in vacuum. The computation of the nodal capacitance matrix and the inductance matrix is based on [35].

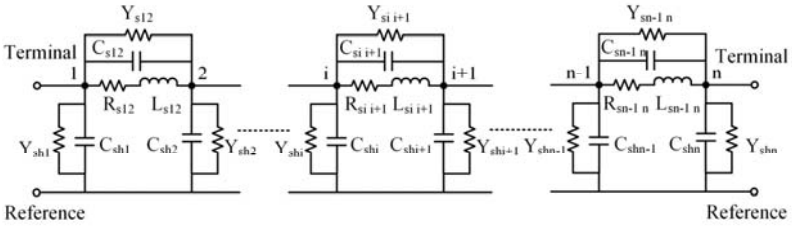

Figure 1. The equivalent circuit of the transformer winding model represented by "n" identical blocks. The mutual coupling between the blocks is not shown for simplicity.

D. *Linearization of the matrix of voltage distribution factors*

The most heavy computation load in the above model is focused on the computation of the voltage distribution matrix. The winding model in Fig.1 is topologically invariant. In addition, the dependency of the elements of the voltage distribution matrix follows the same pattern no matter what the angular frequency spectrum is [34]. However, although the pattern remains the same, because the frequency spectrum of the input voltages depends on each particular switching event behaviour, the elements of the voltage distribution matrix must be computed accordingly. This is computationally costly and from modelling perspective means that one does not efficiently use the advantage of the above characteristics of invariance of the model.

In order to take full advantage of the invariance characteristics of the model, the voltage distribution matrix is linearized by following the method of linear interpolation. Let us suppose a primitive vector of angular frequencies $\left[\omega_k^p\right]$ for which $\omega_k^p \in \left[\omega_{\min}^p,\ \omega_{\max}^p\right]$ and all discrete values differ a constant angular frequency step $\Delta\omega^p$. By using the vector $\left[\omega_k^p\right]$, the corresponding primitive vectors of (n-2)x1 for the voltage distribution factors when the input is at the terminals "1" and "n", respectively, as $\left[T_{i,1}^p\left(\omega_k^p\right)\right]$ and $\left[T_{i,n}^p\left(\omega_k^p\right)\right]$, are considered to be known for all the values in $\left[\omega_k^p\right]$. These primitive matrices are used to define any other $\left[T_{i,1}(\omega)\right]$ and $\left[T_{i,n}(\omega)\right]$ in respect to any vector of angular frequencies $[\omega]$ of a switching event.

By following the linear interpolation approximation, one may derive that the i^{th} elements in $\left[T_{i,1}(\omega)\right]$ and $\left[T_{i,n}(\omega)\right]$ matrices are computed respectively as

$$T_{i,1}(\omega)=\frac{\omega-\omega_k^p}{\Delta\omega^p}\left[T_{i,1}^p\left(\omega_{k+1}^p\right)-T_{i,1}^p\left(\omega_k^p\right)\right]+T_{i,1}^p\left(\omega_k^p\right) \quad (7)$$

$$T_{i,n}(\omega)=\frac{\omega-\omega_k^p}{\Delta\omega^p}\left[T_{i,n}^p\left(\omega_{k+1}^p\right)-T_{i,n}^p\left(\omega_k^p\right)\right]+T_{i,n}^p\left(\omega_k^p\right). \quad (8)$$

In this pattern, the voltage distribution factors $T_{i,1}$ and $T_{i,n}$ are still frequency depended but automatically piece-wise linearized along each particular vector of angular frequencies $[\omega]$ of a switching event.

III. MEASUREMENTS AND RESULTS

The one line diagram of the measuring setup is shown in Fig. 2. For the voltage measurements at transformer terminals, 150 pF capacitive dividers with a ratio of 2500 are used. The voltages are measured by a 22 channel/14 bit transient recorder at 10Msample/s. Cable and load data as well as the switch-on and switch-off operations of the vacuum circuit breaker (VCB) case studies for the conducted measurements are presented in [35]. The supplied by the vacuum circuit breaker (VCB) and the cable core-type three-phase transformer has ratings of 3.75MVA, 36.59/0.65 kV, delta-wye. The primary side windings consist of 13 coils and each coil has approximately 90 foil-type turns. Measuring points exist on transformer terminals, at both HV and LV sides. Additionally, each primary winding is equipped by a special measuring point at the 90$^{\text{th}}$ turn. The most important geometrical parameters of the transformer windings are summarized in Table I. In view of Fig. 1, the 13 coils compose an equivalent circuit of n=14 nodes where nodes "1" and "14" are the terminal input nodes. at transformer terminals and at the 90$^{\text{th}}$ turns of the high voltage (HV) windings.

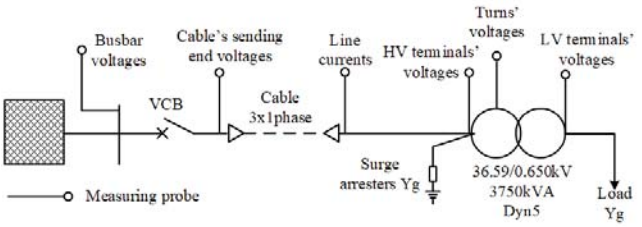

Figure 2. The simplified one line diagram of the measuring setup.

TABLE I. TRANSFORMER DATA

Geometrical data	Low voltage winding	High voltage winding
Turns sum	12	1170
Coils	1	13
Turns per coil	12	90
Inner diameter [mm]	376	655
Outer diameter [mm]	450	751
Strip [mm]	1.600x1200	0.400x71

A dedicated code has been written in Matlab for the computations. The primitive vector of angular frequencies $\left[\omega_k^p\right]$ for which $\omega_{\min}^p = 2\pi 10^{-3}\,\text{Hz}$, $\omega_{\max}^p = 2\pi 10^{7}\,\text{Hz}$ and $\Delta\omega^p = 1000\pi\text{Hz}$. For this vector, the primitive vectors $\left[T_{i,1}^p\left(\omega_k^p\right)\right]$ and $\left[T_{i,n}^p\left(\omega_k^p\right)\right]$ are also computed.

Time-domain voltage measurements at the winding terminals and at the 90th turn in each winding were recorded during three-phase closing and opening operations of the VCB. The measured time domain input terminal waveforms must be transformed in frequency domain in order to define the vector of the angular frequencies $[\omega]$ and the input vector $\left[e_1(\omega)\quad e_n(\omega)\right]^T$ for the computations. When the correct vector of the angular frequencies has been determined, using (7) and (8) the matrix of voltage distribution factors $\left[\left[T_{i,1}(\omega)\right]\ \left[T_{i,n}(\omega)\right]\right]$ is computed and finally the internal voltages are computed using (3). Thereafter, inverse Fourier transform is applied to transfer the results in time-domain. One case of closing operation of the VCB is presented next.

The symmetrical construction of the winding leads to symmetrical impedance matrix. Hence, the matrix $\left[T_{i,n}^p\left(\omega_k^p\right)\right]$ is symmetrical to $\left[T_{i,1}^p\left(\omega_k^p\right)\right]$ and the matrix $\left[T_{i,n}(\omega)\right]$ is symmetrical to $\left[T_{i,1}(\omega)\right]$ [34]. The elements of the 12x1 size matrices $\left[T_{i,1}^p\left(\omega_k^p\right)\right]$ and $\left[T_{i,1}(\omega)\right]$ are presented in the Fig. 3. The elements of the $\left[T_{i,1}(\omega)\right]$ matrix fit very well to the elements of $\left[T_{i,1}^p\left(\omega_k^p\right)\right]$ matrix in the whole frequency spectrum. Hence, the matrices $\left[T_{i,n}(\omega)\right]$ and $\left[T_{i,1}(\omega)\right]$ are valid to be used for further computation of the transient voltage waveforms. The computed internal voltage waveforms for the three windings are presented in Fig. 4. The co-instantaneously measured waveform in the 90th turns are also presented for comparison in the Fig. 5. There is a good agreement between the computed waveforms with the measured waveforms for each of the three windings. In particular, the computed rate of rise of the voltage is in good agreement with the measured rate of rise as well. However, slight differences, observed as noise, are due to the electromagnetic compatibility issues because of the adjacency of many measuring wires. Moreover, differences between computed and measured values are because all measuring points cannot be reached directly onto the turn. A connection between the turn and the outside taps exists which is not reflected into the equivalent circuit in Fig. 1. A detailed analysis of the load influence on the switching transient in the presence of a VCB one can find in [35].

IV. Discussion

For this particular case study, for each particular angular frequency ω_k^p the size of the primitive matrix $\left[T_{i,1}^p\left(\omega_{k+1}^p\right) - T_{i,1}^p\left(\omega_k^p\right)\right]$ is 12x2. That is because we define two

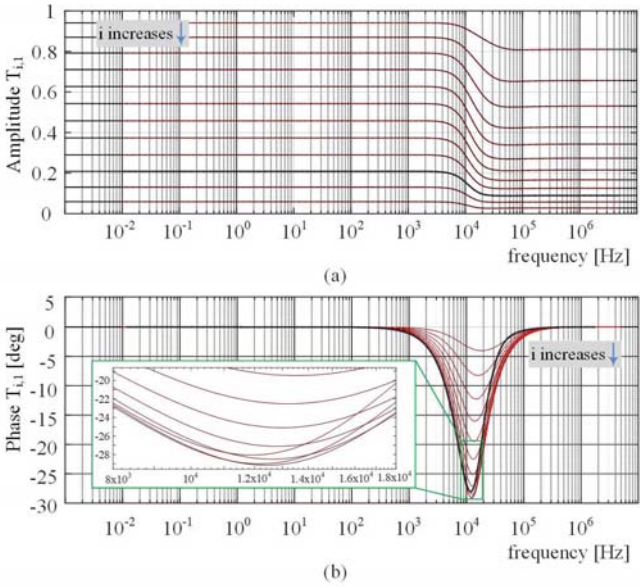

Figure 3. Comparison of the primitive elements (black lines) to the piece-wise linearized elements (red lines) of the twelve $T_{i,1}$ voltage distribution factors in respect to terminal "1": (a) the amplitudes and (b) the phases.

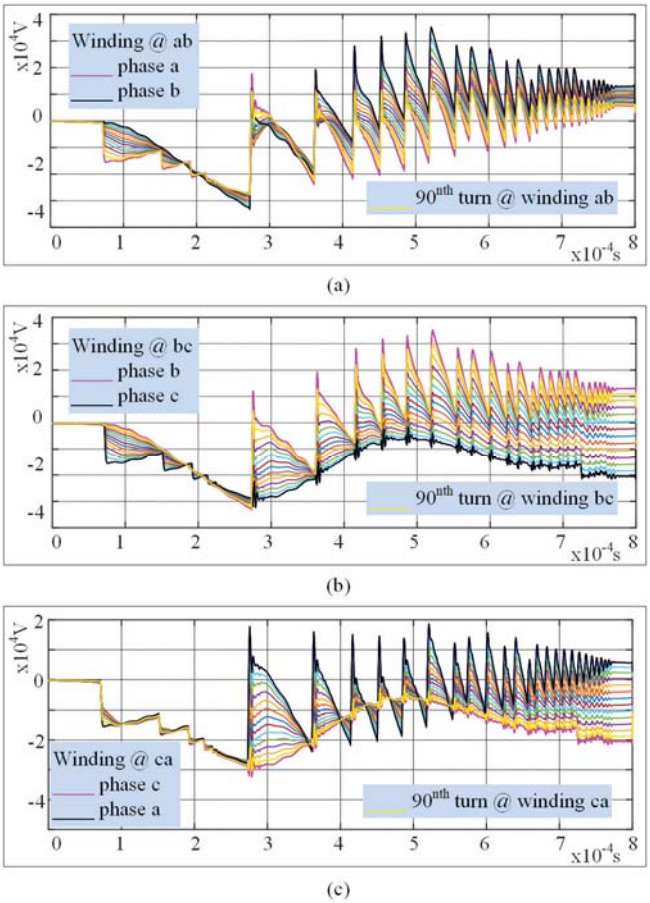

Figure 4. The computed internal voltage waveforms for the winding between: (a) "a" and "b" phases, (b) "b" and "c" phases and (c) "c" and "a" phases. The yellow coloured waveforms shown the measured values in the 90th turns of the windings.

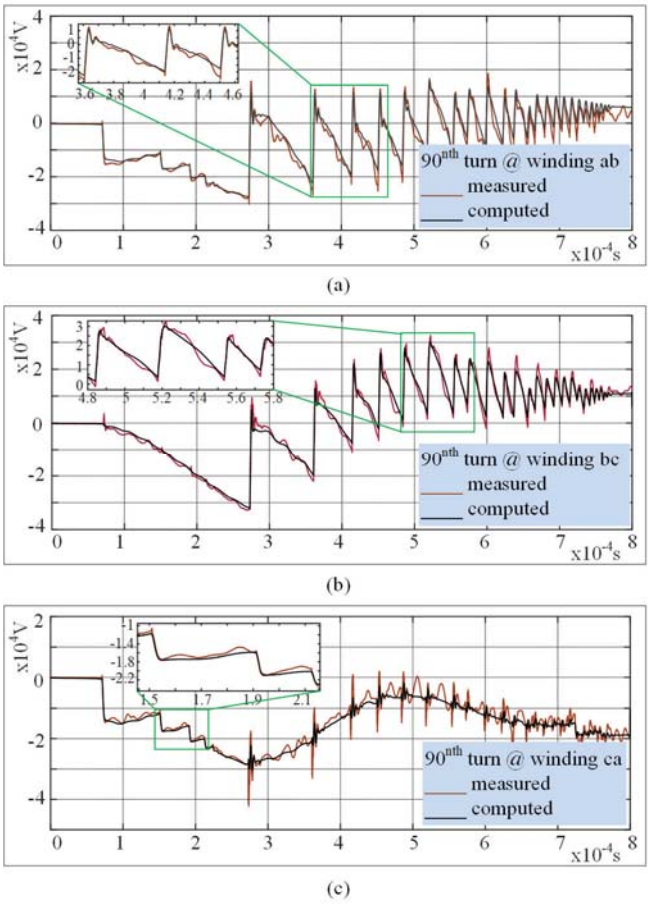

Figure 5. Comparison of the computed voltage waveforms to the measured voltage waveforms for the 90th turns of the windings between: (a) "a" and "b" phases, (b) "b" and "c" phases and (c) "c" and "a" phases.

input terminal nodes for the winding and twelve internal nodes. The number of internal nodes defines the number of rows of the primitive matrix and depends on the discretization of the transformer winding. The elements of the primitive matrix can be determined by using analytical formulas as in this case study. The case of using sweep frequency response analysis is under examination as well. It is also important to consider the sampling step $\Delta\omega^p$. The sampling step defines the number of the factors values at each particular node for the whole frequency spectrum of $\omega_k^p \in \left[\omega_{\min}^p, \omega_{\max}^p\right]$. In this manner, a number of primitive matrices reveals which is equal to the number of elements in the vector $\left[\omega_{\min}^p, \omega_{\max}^p\right]$. In our case study, this is reflected by the 12x2x200.000 three-dimensional matrix, which is easily handled in Matlab. An investigation of the sampling influence on the model performance is under examination too. In this case study, the input terminal voltages at nodes "1" and "14" have been determined by measurements. A suitable black-box transformer model in a future investigation should compute these input voltages. Moreover, the windings connections might be important to be taken into account depending on the formulation of the state equations of black-box transformer model. This conceptual integration of the winding model to the transformer model accommodates the development of a unified transformer model.

V. CONCLUSIONS

In this paper, a robust method for the combination of black box transformer models to suitable lumped-parameters winding models for direct computation of the internal voltage distribution is presented. The successful combination demands fast and direct voltage computations, especially after the computation of the input terminal voltages, as well as the avoidance of parameters determination from geometrical transformer data. The method is based on the linearization of the primitive matrix of the voltage distribution factors. The primitive matrix can be considered as a characteristic quantity for each transformer. It can be computed either by analytical formulas or could be defined by the manufacturer through measurements. The computed from the black box model terminal voltages might be used as inputs on which the linearized matrix of the voltage distribution factors applies and the vector of internal voltages results. The comparison of measured with the computed waveforms verifies the high accuracy of the applied method for analyzing internal transient voltages during switching operations.

REFERENCES

[1] *Electrical Transient Interaction Between Transformer and the Power System, Part-1: Expertise*, Joint Working Group A2/C4.39, Cigre, Apr. 2014.

[2] *Electrical Transient Interaction Between Transformer and the Power System, Part-2: Case Studies*, Joint Working Group A2/C4.39, Cigre, Apr. 2014.

[3] P. Mukherjee and L. Satish, "Construction of equivalent circuit of a transformer winding from driving-point impedance function analytical approach", *IET Electr. Power Appl.*, vol. 6, pp. 172–180, 2012.

[4] B. Gustavsen, "Study of transformer resonant overvoltages caused by cable-transformer high-frequency interaction," *IEEE Trans. Power Del.*, vol. 25, pp. 770-779, Apr. 2010.

[5] B. Gustavsen, A. P. Brede, and J. O. Tande, "Multivariate analysis of transformer resonant overvoltages in powers station," *IEEE Trans. Power Del.*, vol. 26, pp. 2563-2572, Oct. 2011.

[6] B. Badrzadeh and B. Gustavsen, "High-frequency modeling and simulation of wind turbine transformer with doubly fed asynchronous generators," *IEEE Trans. Power Del.*, vol.27, pp.770-779, Apr. 2012.

[7] G. Stein, "A Study of the Initial Surge Distribution in Concentric Transformer Windings," *AIEE Transaction*, pp.877-892, Sept. 1964

[8] M. Popov, R. P. P. Smeets, L. van der Sluis, H. de Herdt, and J. Declercq, "Experimental and theoretical analysis of vacuum circuit breaker prestrike effect on a transformer," *IEEE Trans. Power Del.*, vol. 24, pp. 1266-1274, Jul. 2009.

[9] M. Popov, B. Gustavsen, and J. A. Martinez-Velasco, "Transformer modeling for impulse voltage distribution and terminal transient analysis," in *Electromagnetic Transients in Transformer and Rotating Machines Windings*, 1st ed. Hershey, Pennsylvania, USA.

[10] A. O. Soysal, and A. Semlyen, "Practical transfer function estimation and its application to wide frequency range presentation of transformers," *IEEE Trans. Power Del.*, vol. 8, pp. 1627-1637, Jul. 1993.

[11] B. Gustavsen, and A. Semlyen, "Application of the vector-fitting to the state equation representation of transformers simulation of electromagnetic transients," *IEEE Trans. Power Del.*, vol. 13, pp. 834-842, Jul. 1998.

[12] B. Gustavsen, and A. Semlyen, "Rational Approximation of Frequency Domain Responses by Vector Fitting," *IEEE Trans. Power Del.*, vol. 14, pp. 1052-1061, Jul. 1999.

[13] B. Gustavsen, "Computer Code for Rational Approximation of Frequency Dependent Admittance Matrices," *IEEE Trans. Power Del.*, vol. 17, pp. 1093-1098, Oct. 2002.

[14] B. Gustavsen, "Wide band modelling of power transformers," *IEEE Trans. Power Del.*, vol. 26, pp. 2563-2572, Oct. 2011.

[15] A. Morched, L. Marti, and J. Ottevangers, "A high frequency transformer model for EMTP," *IEEE Trans. Power Del.*, vol. 8, pp. 1615-1626, Jul. 1993.

[16] Y. Shibuya, S. Fujita, N. Hosokawa, "Analysis of Very Fast Transient Overvoltages in Transformer Winding", *IEE Proc Gen. Trans. Distr.*, vol.144, pp.461-468, Sept. 1997.

[17] Y. Shibuya, S. Fujita, E. Tamaki, "Analysis of very fast transient in transformers", *IEE Proc Gen. Trans. Distr.*, vol.148, pp.377-383, Sept. 2001.

[18] M. Popov, L. van der Sluis, G.C. Paap, H. de Herdt, "Computation of very fast Transient overvoltages in transformer windings", *IEEE Trans. Power Del.*, vol. 18, pp. 1268-1274, Oct. 2003.

[19] M. Popov, L. van der Sluis, R.P.P. Smeets, J.L. Roldan, and V. Terzija, "Modelling simulation and measurement of very transients in transformer windings with consideration of frequency-dependent losses," *IET Electr. Power Appl.*, vol. 1, pp.29-35, Jan. 2007.

[20] M. Popov, L. van der Sluis, and R. P. P. Smeets, "Evaluation of surge-transferred overvoltages in distribution transformers," *IET Electr. Power Syst. Res.*, vol. 78, pp. 441-449, 2008.

[21] R. C. Degeneff, "A general method for determining resonances in transformer windings", *IEEE Trans. Power App. Syst.*, PAS-76, pp. 423–430, Mar./Apr. 1977.

[22] P. I. Fergestad, and T. Henriksen, "Transient oscillations in multiwinding transformers," *IEEE Trans. Power App. Syst.*, vol. 93, pp. 500–509, 1974.

[23] A. Miki, T. Hosoya, and K. Okuyama, "A calculation method for pulse voltage distribution and transferred voltage in transformer windings," *IEEE Trans. Power App. Syst.*, vol. PAS-97, pp. 930–939, 1978.

[24] Y. Shibuya, and S. Fujita, "High-frequency model of transformer winding," *Elect. Eng. Japan*, vol. 146, pp. 8-15, 2004.

[25] R. C. Degeneff, W. J. Mcnutt, W. Neugebauer, J. Panck, J., M. E. McCallum, and C. C. Honey, "Transformer response to system switching voltages," *IEEE Trans. Power App. Syst.*, vol. 101, pp. 1457–1470, 1982.

[26] R.C. Dugan, R. Gabrick, J.C. Wright, and K.V Pattern, "Validated techniques for modeling shell-form EHV Transformers", *IEEE Trans. Power Del.*, vol.4, pp. 1070-1078, Apr. 1989.

[27] Y. Yang, Z. J. Wang, X. Cai, and Z. D. Wang, "Improved lumped parameter model for transformer fast transient simulations," *IET Electr. Power Appl.*, vol. 5, pp. 479-485, 2011.

[28] D.J. Wilcox: "Theory of Transformer Modelling Using Modal Analysis," *Proc. Inst. Elect. Eng. C*, vol. 138, pp.121-128, Mar. 1991.

[29] V. Rashtchil, E. Rahimpour, H. Shahrouzi, "Model reduction of transformer detailed R-C-L-M model using the imperialist competitive algorithm", *IET Electr. Power Appl.*, vol. 6, pp. 233–242, 2012.

[30] D. Filipovic-Grcic, B. Filipovic-Grcic, and I. Uglesic, "High-Frequency Model of the Power Transformer Based on Frequency-Response Measurements," *IEEE Trans. Power Del*, vol. 30, pp.34-42, Feb. 2015.

[31] B. Gustavsen and A. Portillo, "A black-box approach to interfacing white-box transformer models with electromagnetic transients programs," *IEEE Power and Energy Society General Meeting*, 6939110, Oct. 2014.

[32] G. H. Oliveira and S. D. Mitchel, "Comparison of black-box modelling approaches for transient analysis: A GIS substation case study," in *Proc. 2013 International Conference on Power Systems Transient 2013,* 2013.

[33] S. D. Mitchel and J. S. Welsh, "Initial parameters estimates and constrains to support gray-box modelling of power transformers" *IEEE Trans. Power Del*, vol. 28, no. 4, pp. 2411 – 2418, Oct. 2013.

[34] A. Theocharis, M. Popov and V. Terzija, "Computation of internal voltage distribution in transformer windings by utilizing a voltage distribution factor," *El. Power Sys. Res.*, vol. 138, pp. 11–17, 2016.

[35] A. Theocharis, M. Popov, R. Seibold, S. Voss and M. Eiselt, "Analysis of switching effects of vacuum circuit breaker on dry-type foil-winding transformers validated by experiments," *IEEE Trans. Power Delivery*, vol. 30, pp. 351 - 359, Feb. 2015.

[36] A. Theocharis and M. Popov, "Modelling of foil-type transformer windings for computation of terminal impedance and internal voltage propagation, " *IET Electr. Power Appl.*, vol. 9, pp. 128–137, 2015.